*Astronomy & Astrophysics* manuscript no. output
July 25, 2019


# The Orbital Surface Density Distribution and Multiplicity of M-Dwarfs

N. Susemiehl[1] and M. Meyer[1,]

Department of Astronomy, University of Michigan, Ann Arbor, MI, USA

June 2019

**ABSTRACT**

*Aims.* We present a new estimate of the multiplicity fraction of M-Dwarfs using a log-normal fit to the orbital surface density distribution.
*Methods.* We used archival data from five M-Dwarf multiplicity surveys to fit a log-normal model of the orbital surface density distribution of these stars. We then used this fit, alongside the companion mass ratio distribution given by Reggiani Meyer (2013), to calculate the frequency of companions over the ranges of mass ratio (q) and semi-major axis (a) that the referenced surveys were collectively sensitive over – [0.60 ≤ q ≤ 1.00] and [0.00 ≤ a ≤ 10,000 AU]. We then extrapolated this to calculate a multiplicity fraction which encompasses [0.00 ≤ q ≤ 1.00] and [0.00 ≤ a < ∞ AU]. Finally, we compared our results to multiplicity findings of other spectral types of stars.
*Results.* Over these constrained region of [0.60 ≤ q ≤ 1.00] and [0.00 ≤ a ≤ 10,000 AU], we found a multiplicity fraction of 0.236 ± 0.061. We then calculated the multiplicity fraction over all ranges of q (0.10 – 1.00) and a (0.00 – ∞ AU) to be 0.475 ± 0.129. We also found evidence which suggests that the multiplicity of M-Dwarfs is identical to that of FGK and A stars over these specific ranges of mass ratio and semi-major axis.

**Key words.** binary stars – M-Dwarfs

## 1. Introduction

M-Dwarfs are among the most numerous stars in the universe, and many exist alongside at least one companion. Numerous attempts have been made to find the multiplicity fraction of M-Dwarfs (Fischer & Marcy 1992, Janson et. al. 2012, Winters 2019), but this value is not yet well constrained. Knowing this value will have important implications for star formation theories, inform us about the emergence of planetary systems around low mass stars, and allow for the modeling of both galactic and extra-galactic stellar populations.

Fundamentally, the multiplicity fraction of a population of stars depends on: 1. the companion mass ratio distribution ($\psi$) and 2. the orbital surface density distribution ($\phi$). The mass ratio, q, is defined as: $\frac{M_{secondary}}{M_{primary}}$ where, by definition, $M_{primary} > M_{secondary}$ so that $q \leq 1$. Furthermore, the semi-major axis, a, of a system serves as a measure of the separation between the primary and secondary stars. Using these two components, we calculate the multiplicity fraction as:

$$f = \int_{q_{min}}^{q_{max}} \psi dq * \int_{a_{min}}^{a_{max}} \phi d log_{10}(a) \quad (1)$$

where $q_{min}, q_{max}, a_{min}$, and $a_{max}$ representing lower and upper bounds for the regions of mass ratio and semi-major axis of interest. The first component, the companion mass ratio distribution, is discussed in Reggiani & Meyer (2013). They find that the formula:

$$\psi = \frac{dN}{dq} = q^{.25 \pm 0.29} \quad (2)$$

describes this distribution for M-Dwarfs and other types of stars. This work has focused on finding the second component to Equation (1), the orbital surface density distribution. Once this is determined, Equation (1) can be used to calculate the multiplicity of M-Dwarfs by integrating over specific ranges of mass ratio and semi-major axis. Our method for calculating the multiplicity fraction is built upon a key assumption: that the mass ratio distribution does not depend on orbital separation. Evidence for this is provided by Reggiani & Meyer (2013).

## 2. Methods

### 2.1. Acquiring the Data

The first step in exploring the orbital surface density distribution and multiplicity of M-Dwarfs was to compile data from a variety of different multiplicity surveys. We utilized data from surveys which employed the radial velocity (Delfosse et. al. (1998), Fischer and Marcy (1992)) and direct imaging (Cortes-Contreras et. al. (2016), Janson et. al. (2012), and Ward Duong et. al. (2015)) companion detection methods. These would later be used as point estimates of the multiplicity fraction for the purposes of fitting a model to the orbital surface density distribution. Incorporating data which arose from these two different detection methods allowed us to investigate companions with broad ranges of semi-major axis. Additional surveys utilizing the microlensing or astrometry detection methods were not used in this analysis because the radial velocity and direct imaging surveys listed above were found to adequately represent the full range of semi-major axis.

Because it covers such a wide range of semi-major axis (3 - 10,000 AU), the data from Ward-Duong et. al. (2015) was split into two bins by orbital separation: 0 - 100 AU and 100 - 10,000 AU. This split is further justified by the fact that the survey utilized two different companion-confirmation methods for these two orbital separation regimes (archival plate analysis and adaptive optics imaging for the near and far separations respectively).

In order to ensure the certainty of companion dectections made by each referenced survey, we sought to constrain our analysis to only include detected multiple systems with the values of mass ratio and semi-major axis to which each survey was at least 90% complete. Collectively, the referenced surveys are complete over the mass ratio range [0.60 ≤ q ≤ 1.00] and the semi-major axis range [0.00 ≤ a ≤ 10,000 AU]. For each survey, any detected companion which did not have associated physical properties of q between 0.60 and 1.00 and the range in a which the specific survey was 90% complete to was removed from our analysis entirely. This removal was done by striking any outlying multiple systems from the data and calculating a multiplicity fraction using the original total population number for each referenced survey. Table (1) below depicts the point estimate of the multiplicity fraction for each survey along with the respective detection method and sensitive range of semi-major axis.

### 2.2. Fitting the Model

Next, we sought to fit a log-normal model to the orbital surface density distribution of the M-Dwarf multiple systems. This model, which we call $\phi$, is described by:

$$\phi = \frac{dN}{dlog_{10}(a)} = A * \frac{e^{-(log_{10}(a)-log_{10}(\mu))^2/(2log_{10}(\sigma)^2)}}{log_{10}(\sigma) * \sqrt{2\pi}} \quad (3)$$

and has 3 free parameters: the base-10 log of mean ($log_{10}(\mu)$), the base-10 log of standard deviation ($log_{10}(\sigma)$), and the amplitude (A). In order to fit the model and find the best values for these parameters, values of the multiplicity were calculated by plugging in possible values of $log_{10}(\mu)$ (ranging from -2 to 5), $log_{10}(\sigma)$ (ranging from -2 to 4), and A (ranging from 0 to 1) into Equation (3) in increments as small as 0.001 and then assuming each iteration of this to be the $\phi$ component of Equation (1) (the $\psi$ is given by Equation (2)). Model multiplicity estimates were then calculated from Equation (1) by integrating the $\psi$ component from 0.60 to 1.00 and the $\phi$ component over the range of semi-major axis associated with each survey. We then compared these model multiplicity estimates to the estimates of multiplicities from the surveys via the reduced-chi squared test. The 6 data points and 3 free parameters lead to 3 degrees of freedom for this test. The best fit model to this distribution allowed us to performs further calculations.

### 2.3. Calculating the Frequency

Next, we used our model for the orbital surface density distribution alongside the companion mass ratio distribution model from Reggiani and Meyer (2013) to calculate the multiplicity of M-Dwarfs as:

$$f = \int_{q_{min}}^{q_{max}} q^{25} dq * A * \int_{a_{min}}^{a_{max}} \frac{e^{-(log_{10}(a)-log_{10}(\mu))^2/(2log_{10}(\sigma)^2)}}{log_{10}(\sigma) * \sqrt{2\pi}} dlog_{10}(a) \quad (4)$$

This formula was first integrated over the ranges of q and a that encompass the survey data: 0.6 ≤ q ≤ 1.0 and 0.00 ≤ a ≤ 10,000 AU. This calculation resulted in a multiplicity fraction that is representative over these limited ranges of q and a. These ranges were later expanded to [0.0 ≤ q ≤ 1.0] and [0 ≤ a < ∞ AU] to allow for the calculation of a universal M-Dwarf multiplicity fraction. The error on the multiplicity fraction was calculated as the 90% confidence interval of the probability distribution function of the multiplicity fraction.

## 3. Results

### 3.1. Orbital Surface Density Model

The best-fit to point estimates of frequency from the five M-Dwarf surveys resulted in the parameters of $log_{10}(\mu)$, $log_{10}(\sigma)$, and A being 1.582, 0.946, and 0.629 respectively. This fit returned a reduced chi-squared parameter value of 2.137. With 3 degrees of freedom, the chi-squared probability distribution indicates that the probability of achieving a value greater than or equal to 2.137 is 0.093. Despite this low probability, we do not reject the null hypothesis that the data came from this model because it exceeds the 0.05 significance level. This indicates that our model is a weak fit to the data but can still be used to understand the physical processes at play. The log normal model with the best-fit parameter values of $log_{10}(\mu)$, $log_{10}(\sigma)$, and A, shown in Figure (1), best describes the orbital surface density distribution of M-Dwarfs, assuming that this distribution is in fact log-normal in the semi-major axis.

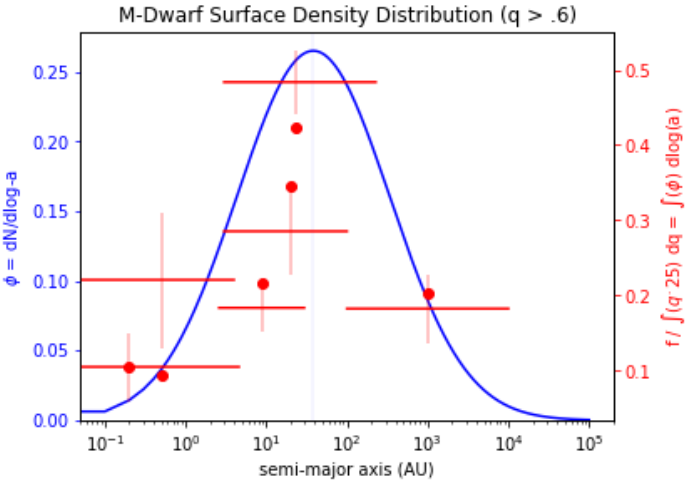


**Fig. 1.** This figure depicts our fit to the orbital surface density distribution of M-Dwarf multiples with mass ratios greater than 0.6. The left axis and blue curve visualize the best fit log-normal model, described by Equation (3) and the best fit parameters given in Section (3.1). The right axis and red features represent the multiplicity estimates calculated from the survey data and our model's attempt to recover these. The y-axis value of each horizontal line represents the multiplicity estimates from the surveys, and the x-axis range represents the range in semi-major axis that each survey is sensitive to. The vertical lines represent the Poisson counting errors of the corresponding survey frequency estimates. Integrating the blue curve over the range of semi-major axis covered by any given red horizontal line results in values represented by the red points. These points visually represent how well our model fits the data.

### 3.2. Multiplicity Fraction

Integrating Equation (4) over the constrained regions of [0.60 ≤ q ≤ 1.00] and [0 ≤ a ≤ 10,000 AU] resulted in a multiplicity

Table (1): Point estimates of multiplicity fraction, q > 0.6

| Reference | Detection Method | Semi-Major Axis Range (AU) | Multiplicity Estimate |
|---|---|---|---|
| Delfosse et. al. (1998) | RV | 0.00 - 4.63 | 0.04 |
| Fischer & Marcy (1992) | RV | 0.04 - 4.00 | 0.08 |
| Cortes-Contreras et. al. (2016) | DI | 2.60 - 29.5 | 0.07 |
| Janson et. al. (2012) | DI | 3.00 - 227 | 0.18 |
| Ward-Duong et. al. (2015) A | DI | 3 - 100 | 0.11 |
| Ward-Duong et. al. (2015) B | DI | 100 - 10,000 | 0.07 |

**Table 1.** This table depicts each of the M-Dwarf surveys used in this study alongside their respective detection method (RV for radial velocity and DI for direct imaging), the range of semi-major axis which the survey was at least 90% complete, and the point estimate of the multiplicity that we made after excluding companion detections outside the respective semi-major axis range and with q < 0.6.

fraction of 0.236 ± 0.061. Following this process, a broad multiplicity fraction was found by integrating Equation (4) over [0.1 ≤ q ≤ 1.0] and [0.0 ≤ a < ∞ AU] to be 0.475 ± 0.129. This broad multiplicity fraction considers stellar and sub-stellar companions to M-Dwarfs, but not planetary companions.

## 4. Discussion

### 4.1. The Multiplicity of M-Dwarfs

The results of our work suggest that around half of all M-Dwarfs have a companion. Because our estimate encompasses very small mass ratios, many of these companions may be Brown Dwarfs.

We sought to compare our model to the to the prediction of Bowler et. al. (2015), which estimated the frequency of Brown Dwarf companions to M-Dwarf hosts (which translates in this work to a low values of mass ratio). They predict the frequency of Brown Dwarf companions to M-Dwarf primaries over a semi-major axis range of 10 - 100 AU and mass ratio range of 0.039 - 0.224 to be $0.028^{+0.024}_{-0.015}$. We integrated Equation (1) with the best fit parameters described above over these ranges of semi-major axis and mass ratio and obtained an multiplicity estimate of 0.0277 ± 0.0093, which is within error of the result from Bowler. The proximity of our results with those of Bowler et. al. (2015) helps enforce the validity of our model.

### 4.2. Comparisons to Other Spectral Type Multiplicities

We sought to compare the multiplicity of M-Dwarfs to that of the sun-like FGK and more massive A type stars over the constrained range of mass ratio and semi-major axis (0.6 ≤ q ≤ 1.0 and 0.00 ≤ a ≤ 10,000 AU). To compare to the FGK multiplicity, we extrapolated the model of orbital surface density from Raghavan et. al. (2010) to integrate over the above range of a. This, alongside the companion mass ratio distribution described in Equation (2) and the full multiplicity equation, Equation (4), was used to find an FGK star multiplicity fraction of 0.230 ± 0.032, where the error is estimated as the Poisson counting error based on the survey of Raghavan et. al. (2010). We used the same method for the A star multiplicity fraction, this time referencing De Rosa et. al. (2013), and found a multiplicity fraction of 0.238 ± 0.026.

In summary, we find the multiplicity fraction over [0.60 ≤ q ≤ 1.00] and [0.00 ≤ a ≤ 10,000 AU] for M, FGK, and A stars to be 0.236 ± 0.061, 0.230 ± 0.032, and 0.238 ± 0.026 respectively. We note that these three values are all within error of one-another, suggesting that the multiplicity fraction does not vary strongly with spectral type. Future studies may explore the multiplicity fraction of OB type stars and Brown Dwarfs to see if this trend holds with the most massive stars and smaller sub-stellar objects.

*Acknowledgements.* We thank the Formation and Evolution of Planetary Systems group for their consistent support. We also thank Dr. Max Moe and Dr. Kimberly Ward Duong for their insightful advice.

## References

Bowler et. al. 2015, Cortes Contreras et. al. 2016 , Astro. & Astrophys., FC23
De Rosa et. al. 2013, Mon. Not. R. Astro. Soc. 437, 1216 1240
Delfosse et. al. 1998, Astro. & Astrophys., 344, 897 910
Fischer and Marcy 1992, The Astrophys. Journal, 396, 178 194
Janson et. al. 2012, The Astrophys. Journal, 754, 44 70
Raghavan et. al. 2010, The Astrophys. Journal , 190, 1 42
Reggiani and Meyer 2013, Astro. & Astrophys., 553, A124
Ward Duong et. al. 2015, Mon. Not. R. Astro. Soc . 000, 1 34 Winters et. al. 2019,